# Negative capacitance regime in antiferroelectric $PbZrO_3$

J. Doherty,[1] K. A. Lynch,[1] and I. Ponomareva[1]

[1] *Department of Physics, University of South Florida, Tampa, Florida 33620, USA*[*]

## Abstract

The potential of antiferroelectrics to exhibit negative capacitance regime has been largely overlooked as all the attention focused on their polar counterparts, ferroelectrics. We use nonequilibrium first-principles-based molecular dynamics to probe negative capacitance regime in prototypical antiferroelectric $PbZrO_3$. Simulations predict that this antiferroelectric can exhibit a negative capacitance/susceptibility regime in response of polarization to *internal* electric field, which is a superposition of applied and residual depolarizing fields. Consequently, the regime emerges when the polarization surface charge in the polar phase of antiferroelectric is not fully screened, as is often the case in thin films and nanostructures. The negative capacitance regime occurs below the Curie temperature and disappears in the paraelectric phase. We find that the time the material spends in the negative capacitance regime is proportional to the time needed to complete antipolar-polar (or its reverse) transition and shortens as the frequency of the applied field increases. Moreover, negative susceptibility value exhibits strong dependence on the quality of surface charge screening with the largest in magnitude values occurring in the vicinity of the transition into negative capacitance regime.

[*] iponomar@usf.edu

## I. INTRODUCTION

Negative capacitance (NC) regime is associated with a decrease in the voltage of a capacitor as charge is added to it [1, 2]. It is under active investigation [3–8], owing to the promise of improving the performance of field effect transistors (FET) through overcoming the Boltzmann tyranny, which places a fundamental limit on the power dissipation of conventional transistor technology [1, 2]. One promising class of materials for such applications are ferroelectrics [9], that is the materials that exhibit spontaneous polarization. Several mechanisms have been proposed in the literature to access NC regime in ferroelectrics and are reviewed in Ref. 9. Some examples are incipient ferroelectric NC regime realized by the incomplete screening of the polarization bound charges that would produce a depolarizing field which stabilizes paraelectric phase below the Curie temperature [9]. Practical realization is in capacitors connected in series [1]. Experimental proof-of-concept NC demonstration was reported in Ref.[10], and latter on the effect has been demonstrated in a ferroelectric [11]. First-principles-based simulations have predicted that the negative susceptibility regime due to residual depolarizing field can be realized even in ferroelectric phase of films [12–14]. In this case susceptibility to internal field could be negative while susceptibility to applied electric field remains positive. Another example is transient NC in ferroelectrics where temporary reduction of voltage upon charge increase is possible as during slowed down delivery of screening charge [9]. First-principles-based simulations predicted that even under nonequilibrium conditions and when the field rate application is extremely high a ferroelectric does not enter thermodynamically forbidden region of negative susceptibility to the applied electric field [14], while susceptibility to internal field could become negative in the presence of residual depolarizing field. Another first-principles-based computational study has predicted negative dielectric permittivity that can occur in different materials when polarization exhibits postswitching oscillations [15]. NC in a model system of multidomain ferroelectric–dielectric superlattices across a wide range of temperatures, in both the ferroelectric and paraelectric phases, has been reported in $PbTiO_3/SrTiO_3$ superlattices [16]. Likewise in $SrTiO_3/PbTiO_3$ superlattices, the local regions of steady-state negative capacitance have been demonstrated experimentally and complemented by phase-field and first-principles-based simulations [17]. More recently, NC regime has been suggested in vdW layered ferroelectric $CuInP_2S_6$ [18]. Through DFT and piezoresponse force

microscopy, it was shown that Cu ion mobility across the vdW gaps results in a NC. On the other hand, the regime of NC in antiferroelectrics, which are antipolar counterparts of ferroelectrics, has received much less attention so far. The static and transient NC effects have been recently demonstrated in proof-of-concept experiment on antiferroelectric $PbZrO_3$ films [19]. The capacitance enhancement due to the static NC effect was observed in a-$HfO_2$/$PbZrO_3$ bilayer capacitor at room temperature, while transient NC was demonstrated across a Pt/$PbZrO_3$/LSMO capacitor in series with a resistor while under pulsed voltage measurements [19]. Hoffman et al. have also reported NC in antiferroelectric $ZrO_2$ by subjecting a $ZrO_2$/$Al_2O_3$/$HfO_2$ capacitor heterostructure in series with a resistor to pulsed electrical measurements [20]. It was concluded that $ZrO_2$ exhibits NC behavior through a structural phase transition from a non-polar to polar state. FET integrated with 10 nm $HfO_2$-based antiferroelectric and ferroelectric heterostack was predicted to achieve performance at par with classical transistors at significantly lower voltage, thanks to NC regime [21]. However, the first-principles-based insight into NC in antiferroelectrics is presently unavailable.

Figure 1(a) shows schematic view of the free energy of an antiferroelectric. The global minimum is associated with antipolar phase, while the two local minima are the polar metastable phases which can be stabilized by the application of an electric field and gives origin to the characteristic double loops. Minimizing the free energy in the presence of electric field yields the equation of state given in Fig 1(b). The shaded region indicates the regime associated with negative susceptibility, that is the region where the system is thermodynamically unstable. The fundamental question is whether antiferroelectrics can enter this region and, if yes, under what conditions? Motivated to answer this question we carry out first-principles-based molecular dynamics (MD) simulations on prototypical antiferroelectric $PbZrO_3$ with the aims (i) to predict the existence of negative susceptibility (NC) regime in this material; (ii) to reveal its origin; (iii) to explore the tunability of such regime in antiferroelectrics.

## II. METHODOLOGY

To reach our aims we simulate $PbZrO_3$ bulk and a 40 nm thin-film using classical MD with the interactions modeled by the first-principle effective Hamiltonian of Ref. 22. The

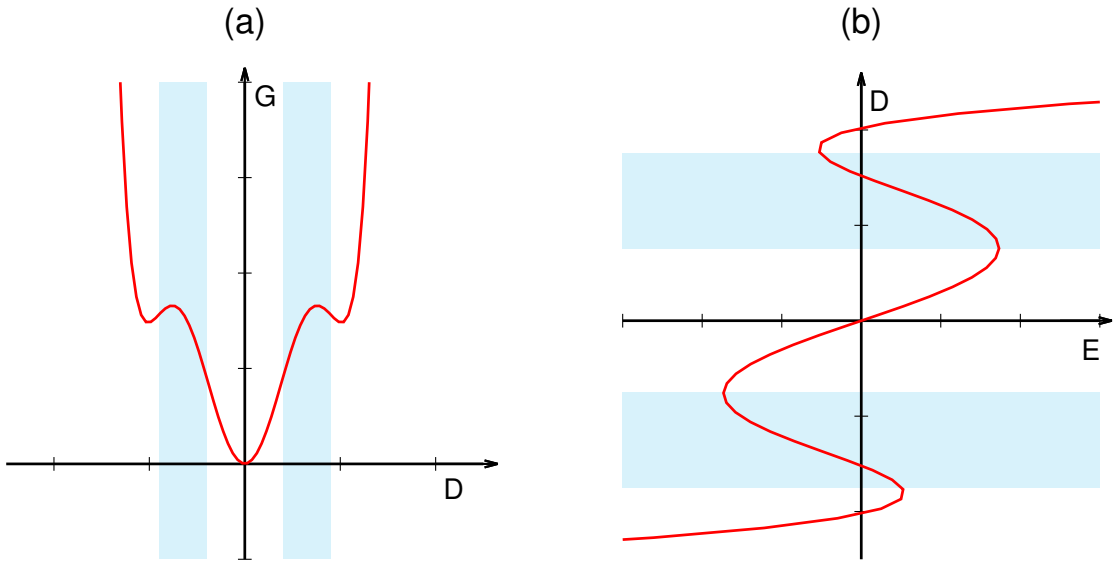


FIG. 1. Schematization of the free energy profile in an antiferroelectric (a) and of the associated equation of state (b).

degrees of freedom for the effective Hamiltonian include polar local modes, $\mathbf{u}_i$, which are proportional to the local dipole moment in the unit cell $i$ and describe the antiferroelectric instability at $\Sigma_2$ point of the Brillouin zone, antiferrodistortive local modes, $\mathbf{w}_i$, that describe oxygen octahedra tilts about Cartesian axes and are responsible for the $R_4$ point instability, and inhomogeneous and homogeneous strain variables, which describe elastic deformations of the unit cell and supercell, respectively. The Hamiltonian includes energy associated with the antiferroelectric $\Sigma_2$ mode and contains contributions from the dipole-dipole interactions, short-range interactions, and on-site self-energy. It also includes energy due to the antiferrodistortive mode that is similar to the previous one but excludes the dipole-dipole interactions as antiferrodistortive local modes are nonpolar. Finally, the Hamiltonian includes the energy associated with elastic deformations. All degrees of freedom are coupled with each other by the symmetry allowed interactions. Simulation of an external electric field is achieved by adding a term to the effective Hamiltonian that couples electric dipoles with the electric field. All parameters of the effective Hamiltonian are derived from density functional theory based computations [22]. This Hamiltonian correctly reproduces the sequence of phase transitions in $PbZrO_3$, its electrical properties, behavior under pressure [22] and mode dynamics [23]. It has previously been used to simulate both bulk and low-dimensional

$PbZrO_3$ structures and in both static and dynamic settings [22–26]. In this study bulk $PbZrO_3$ was simulated by supercell of 20x20x20 perovskite unit cells with periodic boundary conditions applied along all three Cartesian directions. The film was simulated using 12x12x100 supercell of perovskite unit cells with periodic boundary conditions applied along in-plane directions only using the computational approach of Ref. [27]. For the film we simulate partial screening of surface charge using the computational approach of Ref. [27], which computes depolarizing field at an atomistic level. Technically, the amount of surface charge compensation is controlled by a screening parameter $\beta$ that can take values from 0% surface charge screening to 100% surface charge screening. We simulate $NPT$ ensemble with the temperature control achieved via Evans-Hoover thermostat [28]. Integration step for numerical solving of Newton equations of motion was set to 1.0 fs. We simulated the following temperatures of 200, 300, 400, 700, 800, 900, and 1000 K. Note that the computational Curie temperature of $PbZrO_3$ is 946 K [22]. In order to investigate the response of the simulated samples to the electric field, we model the application of *ac* electric field with amplitude of $10\,\mathrm{MV\,cm^{-1}}$ and frequencies of 1.0 to 10.0 GHz in steps of 1.0 GHz. The field was applied along either [001] or [111] pseudocubic crystallographic directions. For each frequency we simulated 15 periods of the *ac* field and then averaged the data over the periods.

## III. RESULTS AND DISCUSSION

In Fig.2(a) the red line presents our computational data for the polarization response of bulk $PbZrO_3$ to the applied electric field, $\mathbf{E}_{app}$, of frequency 5.0 GHz and direction [111]. It has the typical double loop structure. To investigate whether the negative susceptibility regime can be induced by the residual depolarizing field similar to the case of ferroelectrics, we first introduce such field in our modeling indirectly. If the fraction of surface charge screened is $\beta$ then the residual depolarizing field is $\mathbf{E}_{dep} = -\frac{4\pi\mathbf{P}(1-\beta)}{\epsilon_0\epsilon_\infty}$, where $\mathbf{P}$ is the polarization, and $\epsilon_\infty$ is the optical dielectric constant of the material. The total electric field inside the sample, termed the internal field, $\mathbf{E}_{int}$, is now the superposition of the applied field and residual depolarizing field. The associated response of the polarization to the internal electric field is given in Fig.2(a) by black and blue lines and suggests the emergence of negative susceptibility region. Qualitatively similar results were obtained when the field was applied in the [001] direction. Note, that such indirect modeling does not capture the

response of the supercell to the residual depolarizing field, which can vary from the decrease in the polarization magnitude to the disappearance of net polarization altogether. Therefore, our next step is to simulate film in the presence of residual depolarizing field. Figure 2(b)-(c) presents our data for the polarization response in the film to both applied, and internal electric field computed for different percentage of surface charge compensation. Note, that the internal field is computed at an atomistic level, owing to the atomistic treatment of the depolarizing field [27]. The internal field is a superposition of the homogeneous applied field and (partially screened) atomistic depolarizing field. The latter is computed as the gradient of energy penalty associated with the existence of the field in a given nanostructure. At the technical level, the penalty is the difference of the electrostatic energies between the given dipole configurations in film (ideal open circuit boundary conditions) and in bulk (ideal short circuit boundary conditions). The energy penalty contains contributions from every local dipole in the supercell, yielding atomsitic resolution. From Fig. 2(b) we find that the response of the polarization to applied electric field does not exhibit negative susceptibility regime similar to the case of ferroelectrics [14]. As the percentage of surface charge screening decreases polarization reduces, while the coercive field increases. The latter is in contrast to ferroelectrics, where depolarizing field is known to reduce the coercive field [29–31]. Figure 2(c) shows the response of polarization to the internal fields which reveals that, indeed, the negative susceptibility regime occurs for all considered cases of partial surface charge screening, that is $\beta < 1.0$, with the negative slope becoming steeper as $\beta$ decreases. Qualitatively similar data were obtained in simulations for [001] direction of applied electric field. Therefore, we conclude that the negative susceptibility regime emerges in antiferroelectrics under residual depolarizing field in the response of the polarization to the internal electric field, which does not violate thermodynamic stability requirements [13]. Figure 2(d) shows the time evolution of applied, depolarizing and internal fields, and of the polarization. Firstly, we notice that the internal field is significantly lower in magnitude than the applied one, and is occasionally in the opposite direction. Secondly, the fraction of time that the system spends in the NC regime is very small, on the order of a ps. This time is, in fact, limited by the time that it takes the system to complete polar-antipolar (or its reverse) transition. In the NC regime the decrease (increase) in polarization causes increase (decrease) in the internal field. In the classic concept of NC such behavior is attributed to the crossing of the energy barrier [see Fig. 1(a)] through complete annihilation of polarization in a spatially

homogeneous way. However, such concept does not apply in our case as $P(E_{int})$ does not have to follow the the equation of state given in Fig.1(b). From Fig.2(d) we can see that the NC regime is associated with extremely high rate of the depolarizing field demise. This causes temporary enhancement of the internal field, which gives origin to the NC regime.

To predict whether the NC regime can occur in a range of temperatures we repeated simulations for temperatures in the range of 200–1000 K. Below Curie temperature the results are qualitatively similar to Fig. 2(b)-(c), which allows for conclusion that the negative susceptibility regime persists in the antiferroelectric phase. Figure 3(a) shows how hysteresis loops evolve as the temperature approaches the Curie point of the bulk. The area of the loop shrinks, which reduces the region associated with negative susceptibility. At the Curie point and above the negative susceptibility region ceases to exist.

Next we aim to find out whether the NC regime is tunable by the frequency of the electric field. Can the effect disappear above or below certain frequency? Can we extend the time and/or electric field range that the system spends in the NC regime by varying the electric field frequency? For that we repeat simulations for frequencies 1.0 to 10.0 GHz with the step of 1.0 GHz. Hysteresis loops for different frequencies are presented in Fig. 3(b). We find that the NC regime persists in the entire range of frequencies, however, no trend in the $P(E_{int})$ dependencies as a function of frequency is discerned. For frequencies 2.5, 5.0 and 10.0 GHz we computed the average time that the film spends in the NC regime (see shaded areas in Fig.2(d)) and found the values of 1.38±0.15, 1.13±0.11 and 0.77±0.07 ps, respectively. Simulations show that NC regime persists during nearly entire time that it takes the film to complete polar-antipolar (or antipolar-polar) transition, and, therefore, is proportional to this time. As the latter time can vary as a function of *ac* field frequency, this explains why higher frequencies lead to shortened time in the NC regime.

Finally, we assess the tunability of the negative susceptibility to the internal field, $\kappa^{int}$, by the quality of surface charge screening. For that we computed the slope $\kappa^{int}_{E_c} = \left(\frac{\partial P}{\partial E_{int}}\right)_{E_c}$ at each two of the coercive fields $E_c$ associated with polar-antipolar transitions and averaged the data. Thus averaged values, denoted as $\bar{\kappa}^{int}_{E_c}$, as a function of $\beta$ are shown in Fig. 3(c) and reveal strong dependence of the internal susceptibility on the quality of the surface charge screening. The susceptibility increases in magnitude by an order as we approach ideal short circuit boundary conditions. In order to understand this trend we examine hysteresis loops given in Fig.2(c). As $\beta$ increases the slope at the coercive field changes from

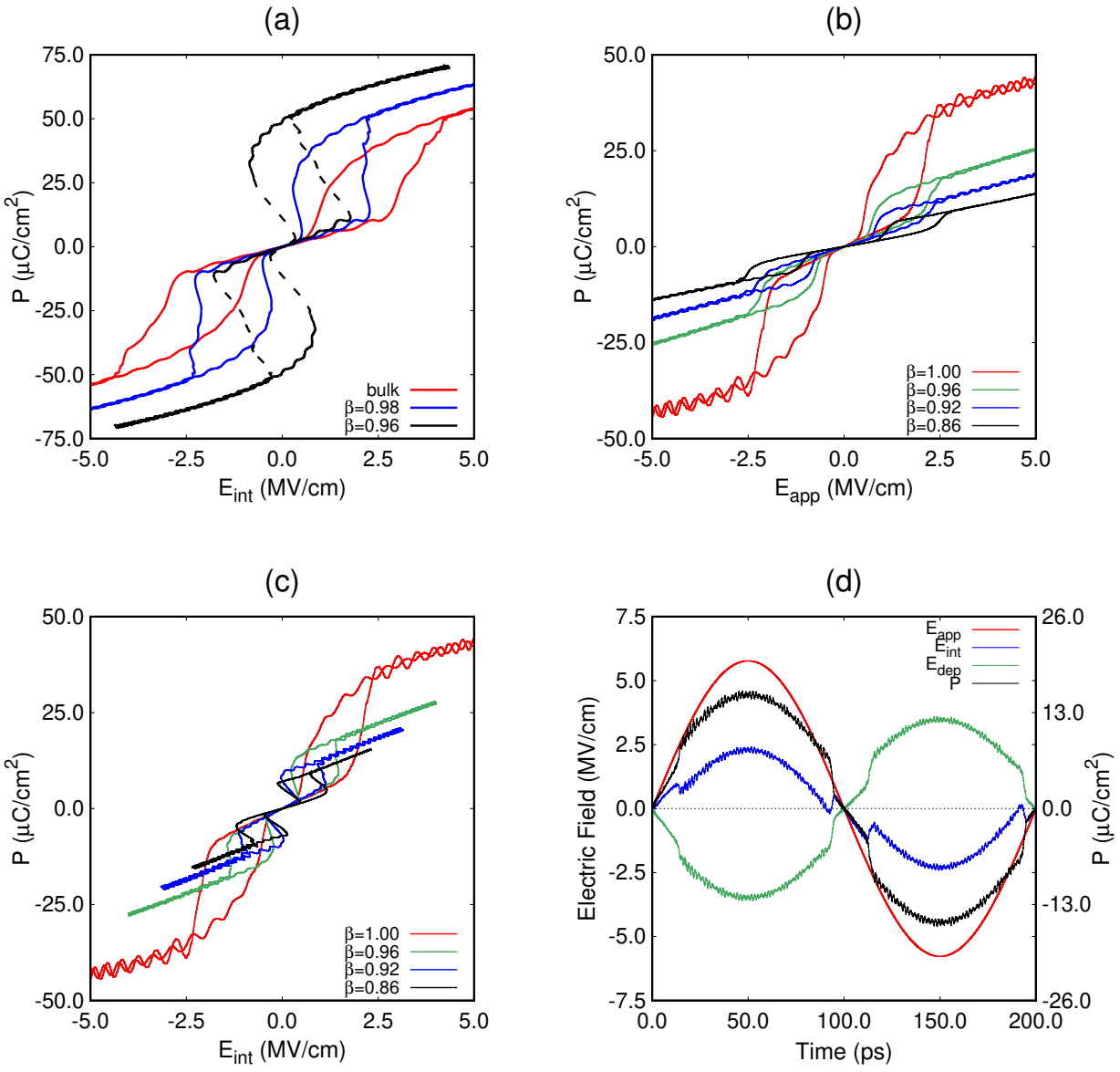


FIG. 2. Hysteresis loops obtained for bulk $PbZrO_3$(a); and for $PbZrO_3$ thin film with respect to both applied (b) and internal electric field (c) computed at 300 K. Note, that for the data for bulk given in panel (a) $E_{int} = E_{app}$ and dashed lines indicate regions of negative capacitance. Time evolution of different fields and polarization component along the growth direction (d). Shading indicates NC regions. The applied electric field frequency is 5 GHz and direction is [111].

negative to positive. Consequently, during this evolution the slope becomes nearly vertical, approaching infinity in value. This occurs at $\beta$ =0.98 and explains the strong enhancement of $\bar{\kappa}^{int}_{E_c}$ at that point. Although this particular $\beta$ is not shown in Fig.2(c), the closest value

of 0.96 demonstrates how the slope approaches a vertical line. This finding also reveals that divergence of internal susceptibility signals the transition into NC regime. From applications standpoint it may be advantageous to have lower values of $\bar{\kappa}^{int}_{E_c}$ to maximize the decrease in voltage upon charge addition. Note that the role of the screening parameter $\beta$ can be related to the capacitance of the dielectric layer, $C_d$, in the "capacitors in series" model [1]. Low $\beta$ correspond to small $C_d$ values (dielectrically stiff material), which suppress polarization [9]. Consequently, we expect enhancement of the internal susceptibility when $C_d$ approaches that of the ferroelectric capacitor. Our simulations carried out for the electric field applied along [001] pseudocubic direction revealed that all the conclusions drawn on the basis of [111] field direction calculations hold. We only find quantitative differences, which allows us to conclude that our qualitative findings are independent of the applied field direction.

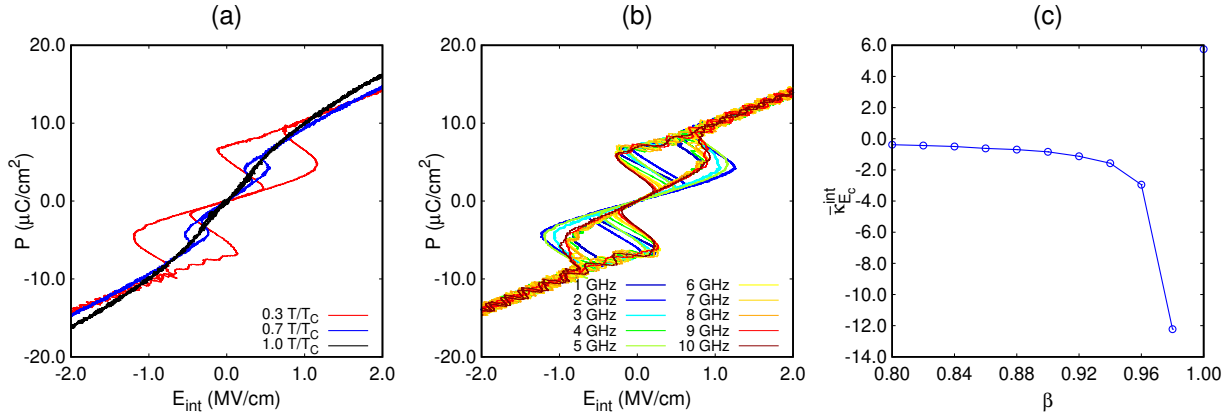


FIG. 3. Polarization as a function of internal electric field for thin film with $\beta = 0.86$ subjected to *ac* electric field of 5.0 GHz frequency at different temperatures (a); and for the same film but at temperature 300 K while subjected to fields of different frequencies (b). In (a) $T/T_C$ is the ratio of temperature to the computational Curie point of bulk $PbZrO_3$. Average susceptibility to internal electric field as a function of surface charge screening parameter computed for the same film at 300 K and under *ac* field of 5.0 GHz frequency (c).

## IV. CONCLUSION

In summary, we used first-principles-based nonequilibrium MD simulation to investigate the regime of negative susceptibility/capacitance and its origin in prototypical antiferroelec-

tric $PbZrO_3$. Under application of *ac* electric field we found that the response of polarization to internal electric field, which is the superposition of applied and depolarizing fields, exhibits negative slope, that is negative susceptibility. In contrast, the susceptibility to applied electric field remains always positive. As the residual depolarizing field was found to be at the origin of the NC regime, this suggests that the experimental route towards such a regime is through depleting screening carriers supply, as indeed is the case in superlattices [16, 17], or when the screening charge is slowed down [11]. The negative susceptibility region is present in the antiferroelectric phase and disappears in the paraelectric phase. Variation of the applied electric field frequency in the GHz range did not reveal trends in the $P(E_{int})$ dependencies. However, we find that the time that film spends in the NC regime shortens as frequency increases. On the other hand, negative susceptibility exhibits strong dependence on the quality of the surface charge screening reaching largest in magnitude values near the value associated with the onset of NC regime.

## V. ACKNOWLEDGEMENTS

This work is supported by the U.S. Department of Energy, Office of Basic Energy Sciences, Division of Materials Sciences and Engineering under grant DE-SC0005245.

[1] S. Salahuddin and S. Datta, Nano letters **8**, 405 (2008).

[2] V. V. Zhirnov and R. K. Cavin, Nature Nanotechnology **3**, 77 (2008).

[3] M. Hoffmann, S. Slesazeck, and T. Mikolajick, APL Materials **9**, 020902 (2021).

[4] M. Hoffmann, M. Gui, S. Slesazeck, R. Fontanini, M. Segatto, D. Esseni, and T. Mikolajick, Advanced Functional Materials **32**, 2108494 (2022).

[5] B. Choudhuri, K. Mummaneni, *et al.*, Journal of Electronic Materials **51**, 923 (2022).

[6] O. Prakash, N. Chauhan, A. Gupta, and H. Amrouch, Microelectronics Journal **115**, 105193 (2021).

[7] M. A. Pavlenko, Y. A. Tikhonov, A. G. Razumnaya, V. M. Vinokur, and I. A. Lukyanchuk, Nanomaterials **12**, 75 (2021).

[8] L. Tu, R. Cao, X. Wang, Y. Chen, S. Wu, F. Wang, Z. Wang, H. Shen, T. Lin, P. Zhou, *et al.*, Nature communications **11**, 1 (2020).

[9] J. Íñiguez, P. Zubko, I. Luk'yanchuk, and A. Cano, Nature Reviews Materials **4**, 243 (2019).

[10] A. Islam Khan, D. Bhowmik, P. Yu, S. Joo Kim, X. Pan, R. Ramesh, and S. Salahuddin, Applied Physics Letters **99**, 113501 (2011).

[11] A. I. Khan, K. Chatterjee, B. Wang, S. Drapcho, L. You, C. Serrao, S. R. Bakaul, R. Ramesh, and S. Salahuddin, Nature materials **14**, 182 (2015).

[12] I. Ponomareva, L. Bellaiche, and R. Resta, Phys. Rev. Lett. **99**, 227601 (2007).

[13] I. Ponomareva, L. Bellaiche, and R. Resta, Phys. Rev. B **76**, 235403 (2007).

[14] K. A. Lynch and I. Ponomareva, Phys. Rev. B **102**, 134101 (2020).

[15] S. Prosandeev, C. Paillard, B. Xu, and L. Bellaiche, Phys. Rev. B **101**, 024111 (2020).

[16] P. Zubko, J. C. Wojdeł, M. Hadjimichael, S. Fernandez-Pena, A. Sené, I. Luk'yanchuk, J.-M. Triscone, and J. Íñiguez, Nature **534**, 524 (2016).

[17] A. K. Yadav, K. X. Nguyen, Z. Hong, P. García-Fernández, P. Aguado-Puente, C. T. Nelson, S. Das, B. Prasad, D. Kwon, S. Cheema, *et al.*, Nature **565**, 468 (2019).

[18] S. M. Neumayer, L. Tao, A. O'Hara, M. A. Susner, M. A. McGuire, P. Maksymovych, S. T. Pantelides, and N. Balke, Advanced Energy Materials **10**, 2001726 (2020).

[19] L. Qiao, C. Song, Y. Sun, M. U. Fayaz, T. Lu, S. Yin, C. Chen, H. Xu, T.-L. Ren, and F. Pan, Nature Communications **12**, 1 (2021).

[20] M. Hoffmann, Z. Wang, N. Tasneem, A. Zubair, P. V. Ravindran, M. Tian, A. A. Gaskell, D. Triyoso, S. Consiglio, K. Tapily, *et al.*, Nature communications **13**, 1 (2022).

[21] K. Karda, A. Jain, C. Mouli, and M. A. Alam, Applied Physics Letters **106**, 163501 (2015).

[22] B. K. Mani, S. Lisenkov, and I. Ponomareva, Phys. Rev. B **91**, 134112 (2015).

[23] Z. G. Fthenakis and I. Ponomareva, Phys. Rev. B **96**, 184110 (2017).

[24] B. K. Mani, C.-M. Chang, S. Lisenkov, and I. Ponomareva, Phys. Rev. Lett. **115**, 097601 (2015).

[25] Z. G. Fthenakis and I. Ponomareva, Phys. Rev. B **98**, 054107 (2018).

[26] S. Lisenkov, Y. Yao, N. Bassiri-Gharb, and I. Ponomareva, Phys. Rev. B **102**, 104101 (2020).

[27] I. Ponomareva, I. I. Naumov, I. Kornev, H. Fu, and L. Bellaiche, Phys. Rev. B **72**, 140102 (2005).

[28] D. C. Rapaport, *The Art of Molecular Dynamics Simulation*, 2nd ed. (Cambridge University Press, 2004).

[29] X. Lou, Journal of Physics: Condensed Matter **21**, 012207 (2008).

[30] Y. A. Genenko, J. Wehner, and H. von Seggern, J. Appl. Phys. **114**, 084101 (2013).

[31] M. Kingsland, Z. G. Fthenakis, and I. Ponomareva, Phys. Rev. B **100**, 024114 (2019).